IEEE Access
Multidisciplinary ⋮ Rapid Review ⋮ Open Access Journal

Received January 1, 2020, accepted January 16, 2020, date of publication January 24, 2020, date of current version February 5, 2020.

Digital Object Identifier 10.1109/ACCESS.2020.2969360

Robust Rigid Registration Algorithm Based on Correntropy and Bi-Directional Distance

TENG WAN[1], SHAOYI DU[1], WENTING CUI[1], YANG YANG[1], AND CE LI[2]
[1]Institute of Artificial Intelligence and Robotics, Xi'an Jiaotong University, Xi'an 710049, China
[2]College of Electrical and Information Engineering, Lanzhou University of Technology, Lanzhou 730050, China

Corresponding author: Shaoyi Du (dushaoyi@gmail.com)

This work was supported by the National Natural Science Foundation of China under Grant 61971343 and Grant 61627811.

ABSTRACT Point set registration is a key method in computer vision and pattern recognition. In this paper, the correntropy and bi-directional distance are introduced into registration framework and a new robust registration model for RGB-D data is proposed. Firstly, as registering point sets with smooth structure, such as surface or plane, is easy failed, the color and position information is fused to establish more precise correspondence between two RGB-D data sets. Secondly, to reduce the influence of noises and eliminate outliers, the registration model based on the maximum correntropy criterion is established. Thirdly, the bi-directional distance measurement is introduced into the registration framework to avoid the model being trapped into local extremum. In addition, to solve this new registration problem, a new iterative closest point (ICP) algorithm is proposed, which converges to the local optimal solution by iterations. In the experiments, the proposed algorithm achieves more robustness and precise registration results than other algorithms.

INDEX TERMS Maximum correntropy criterion, point set registration, RGB-D data, iterative closest point, bi-directional distance.

I. INTRODUCTION

Rigid point set registration is commonly used in simultaneous localization and mapping (SLAM) [1], [2], augmented reality (AR) [3], [4] medical image processing [5], [6] and other fields. The purpose of point set registration is to find an optimal rigid transformation to register two point sets tightly. To solve this registration problem, many algorithms have been proposed such as iterative closet point (ICP) [7]–[9], normal distributions transform (NDT) [10], Gaussian mixture models registration, (GMMREG) [11], coherent point drift (CPD) [12], [13], 4 Points Congruent Sets (4PCS) [14], and other registration algorithms. Among them, the ICP algorithm is widely used for rigid registration due to its simplicity, accuracy and speed. Moreover, with the development of imaging technology, some scholars focus on the registration of RGB-D (red, green, blue and depth) data [15]–[17]. In this paper, our work mainly focuses on the problem of registering the RGB-D data based on ICP registration framework.

After decades of research, a large number of variant methods are proposed to improve the speed of ICP registration algorithm. Benjemaa and Schmitt [18] proposed a variant ICP registration algorithm based on a twin z-buffer structure. This method greatly speeds up the searching process of the nearest neighbor points via partition and sparse point sets, and enables the ICP algorithm to quickly establish the correspondences between point sets. Jost and Hügli [19] put forward an improved ICP algorithm with heuristic approach, which reduces computing complexity via local search. During establishing the correspondences between two point sets, this algorithm uses a good approximation of the nearest point, rather than an exact nearest point. This search method is more effective in point set registration based on uniform point distribution, however, the algorithm is prone to errors when the point sets are unevenly distributed. Greenspan and Yurick [20] used approximate k-d tree search method to speed up the standard ICP algorithm. In the process of establishing correspondence of point sets, this method adds some distance boundary constraints to the original k-d tree to strengthen the searching speed. However, if the adjacent point is not within this boundary range, this method returns only approximate results. He et al. [21] presented an improved ICP algorithm based on geometric features of point sets. The surface normal, curvature and density of point sets are introduced into cost

The associate editor coordinating the review of this manuscript and approving it for publication was Xian Sun.

function of standard ICP algorithm to achieve precise correspondences. Since not all points participate in registration, the speed of this algorithm has been greatly improved.

Meanwhile, some researchers focus on improving the precision of registration algorithm. Makovetskii *et al.* [22] proposed a robust point set registration algorithm with point-to-plane approach. Different from the correspondence search method of point-to-point, the loss function of point-to-plane is to minimize the square of the distance from the source vertex to the face where the target vertex is located. Therefore, the optimization of point-to-plane method is a nonlinear problem and the registration robustness is enhanced. Moreover, with the popularization of RGB-D camera, the color information is added into ICP algorithm to upgrade the registration precision via building more exact correspondences. Men *et al.* [23] published a four-dimensional ICP algorithm, which combines color information with coordinate information of point set. When building the correspondences of point sets, this algorithm can achieve precise registration results. However, because all points participate in registration, when the number of points of a certain color is too large or too small, the registration accuracy is reduced. Korn *et al.* [24] gave an improved Generalized-ICP algorithm with the Lab color space information. When finding correspondences between two point sets, a six-dimensional nearest neighbor search method based on a k-d tree is presented. Furthermore, the plane-to-plane search strategy improves the robustness of registration.

Although the above algorithms have achieved significant improvements in the speed and accuracy of registration, they cannot effectively align two point sets when there are noises and outliers in the point sets. Therefore, some researchers have studied the robustness of point set registration and proposed many robust ICP variants. Chetverikov et al. [25] proposed a robust extension of ICP algorithm with trimmed squares. In each iteration process, the number of reserved points is calculated based on the overlap rate according to the ranking of distance residuals, and the transformation is carried out in light of the reserved points. This method can deal with the partial overlap problem well and ICP algorithm is a special case of TrICP algorithm. Du et al. [26] presented an isotropic scaling registration algorithm with feature points. To reach precise registration, the corner point of point set is added into traditional scaling ICP registration framework, so this algorithm can overcome the influence of local transformation on accuracy. However, when there are too many corners in the point set, the registration accuracy is reduced. Wu *et al.* [27], [28] raised a robust scale ICP algorithm based on maximum correntropy criterion. Compared with the least squares optimization strategy in ICP algorithm, correntropy has better convergence. Therefore, correntropy based ICP algorithm has good registration effect even if the point cloud contains noise and outliers.

Although above algorithms have solved the problem with noises and outliers, they are still impossible to register two point sets with smooth or flat structure accurately. Hence, to improve the robustness and accuracy of the registration of RGB-D data, we fuse color and position information of points to search more correct correspondences between two point sets. Then, we integrate the maximum correntropy criterion into registration framework. At last, the bi-directional distance measurement is used to prevent the proposed algorithm from falling into local extremum. The experimental results demonstrate that our algorithm could reach more robust and precise registration results than other methods.

The main contributions of our approach are as follows: 1) the color information of points is fused to the registration model for two point sets establish precise correspondences. This method improves the registration accuracy of point cloud with no obvious structural change; 2) we apply maximum correntropy criterion to reduce the influence of noises and exclude outliers; 3) the bi-direction distance measurement is presented to decrease the possibility of algorithm falling into local extremum.

The other parts of this paper are structured as follows. In section 2, we briefly introduce the ICP based rigid point set registration algorithm. In section 3, our algorithm is proposed. Meanwhile, the use of point cloud color information, maximum correlation entropy and bi-distance measurement are introduced in order. In section 4, we test our algorithm with other rigid registration algorithms in synthetic data and real data. In section 5, the conclusion and contribution of the proposed algorithm are given.

II. RIGID POINT SET REGISTRATION

Rigid point set registration is aimed to register two m-dimensional (m-D) point sets via precise rigid transformation. Supposing there are two point sets in $\mathbb{R}^m$, one is the source point set $X \triangleq \{\overrightarrow{x}_i\}_{i=1}^{N_x} (N_x \in \mathbb{N})$ and another is the target point set $Y \triangleq \{\overrightarrow{y}_j\}_{j=1}^{N_y} (N_y \in \mathbb{N})$. The objective function of rigid registration algorithm is as follows:

$$\min_{\mathrm{R},\overrightarrow{t},c(i)\in\{1,2,\cdots,N_y\}} \sum_{i=1}^{N_x} ||(\mathbf{R}\vec{x}_i + \vec{t}) - \vec{y}_{c(i)}||_2^2$$
$$s.t.\ \mathbf{R}^{\mathrm{T}}\mathbf{R} = I_m, \det(\mathbf{R}) = 1 \quad (1)$$

where $\mathbf{R} \in \mathbb{R}^{m\times m}$ is a rotation matrix, $\vec{t} \in \mathbb{R}^m$ is a translation vector and $c(i)$ is the set of correspondence points. To optimize this least squares (LS) formula and calculate $\mathbf{R}$ and $\vec{t}$, ICP algorithm repeats the following two steps iteratively.

Firstly, we establish correspondences between source and target point sets:

$$c_k(i) = \underset{c(i)\in\{1,2,\cdots,N_y\}}{\arg\min} ||(\mathbf{R}_{k-1}\vec{x}_i + \vec{t}_{k-1}) - \vec{y}_{c(i)}||_2^2, \quad i = 1, 2, \cdots, N_x \quad (2)$$

Secondly, we calculate the rigid transformation $(\mathbf{R}_k, \overrightarrow{t}_k)$ according to the correspondences:

$$(\mathbf{R}_k, \vec{t}_k) = \underset{\mathrm{R}^T\mathrm{R}=I_m,\det(\mathrm{R})=1,\overrightarrow{t}}{\arg\min} \sum_{i=1}^{N_x} ||\mathbf{R}\vec{x}_i + \vec{t} - \vec{y}_{c_k(i)}||_2^2 \quad (3)$$

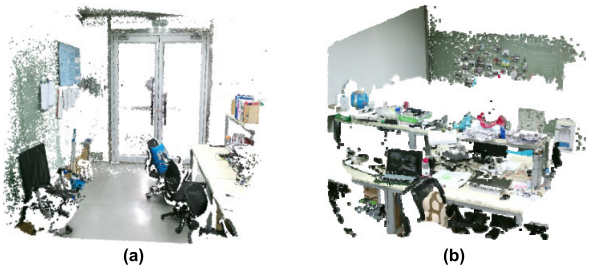

FIGURE 1. RGB-D data. (a) Point set 1. (b) Point set 2.

Due to the limitations of the LS problem, the robustness of traditional ICP algorithm is susceptible to noises and outliers. In addition, because the point set registration is a non-convex optimization problem and ICP algorithm can be trapped in a local extremum sometimes.

III. ROBUST REGISTRATION MODEL FOR RGB-D DATA

A. PROBLEM STATEMENT

Usually, 3-d point sets can precisely reflect the geometry structure and spatial location of object or scene cannot be widely applied for dense point set registration and scene reconstruction. Fortunately, RGB-D camera is designed to generate dense RGB-D point sets via capturing the image and depth data simultaneously. The RGB-D data is shown in Fig.1. Here, the RGB-D data is dense and colorful, but it also contains lots of noises and outliers. Therefore, traditional ICP algorithm cannot register RGB-D point sets well. In addition, the color information of RGB-D point sets is not fully utilized to improve the accuracy of registration. To solve these problems and gain robust RGB-D point set registration, a new ICP based registration algorithm is proposed.

B. ESTABLISHING CORRESPONDENCES WITH COLOR INFORMATION

In traditional ICP algorithm, the correspondences between source and target point sets are established by nearest Euclidean distance. However, when the geometric structure of point set is smooth and uniformly distributed, such as curved and flat surface, using the Euclidean distance alone cannot establish correct correspondences, which is shown in Fig. 2(a). To solve this problem, we introduce the color information into the establishing process of correspondences. Therefore, the nearest distance between two points in source and target point sets should be found in both Euclidean and color space. Moreover, the expected results of establishing correspondence are as shown in Fig. 2(b).

However, in the experiment we found that the color information of points is susceptible to illumination change, which will lead to the establishment of the wrong correspondences. To overcome the impact of illumination, we change the color information of points from RGB color space to HSV (hue, saturation, value) color space. Among them, saturation refers to the vividness of color and value indicates the degree of color brightness. To decrease the impact of illumination, saturation and value need to be deleted and only hue should

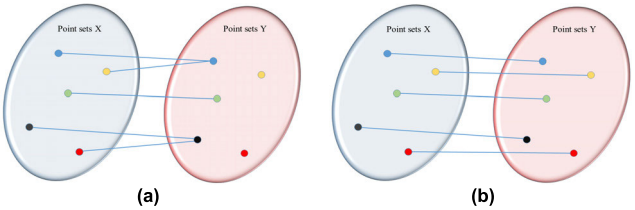

FIGURE 2. Establishing correct correspondences between two points sets via finding the nearest distance in both Euclidean and color space. (a) The wrong correspondences established by the nearest Euclidean distance. (b) The correct correspondences established by the nearest distance in both Euclidean and color space.

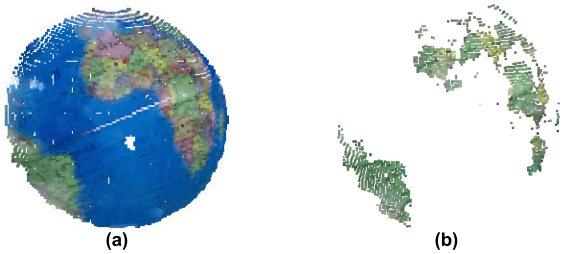

FIGURE 3. Point set selection based on color information. (a) Point set before color screening. (b) Point set after color screening.

be applied. Therefore, when hue is introduced into ICP registration framework, a new objective function is proposed:

$$\min_{\mathrm{R},\vec{T},c(i)\in\{1,2,\cdots,N_y\}} \sum_{i=1}^{N_x}\left(||(\mathbf{R}\vec{x}_i+\vec{t})-\vec{y}_{c(i)}||_2^2+w(h_i^x-h_{c(i)}^y)^2\right)$$
$$s.t.\ \mathbf{R}^{\mathrm{T}}\mathbf{R}=I_m,\ \det(\mathbf{R})=1 \tag{4}$$

where h_i^x and $h_{c(i)}^y$ are hues of source point set and target point set, w is the weight of hue, which is set to 30 according to experience. In addition, point set registration may fail because of the influence of background and noise points. To solve this problem, we classify colors into eight categories based on the value of hue and the specific classification is as follows: red (0–0.0556), orange (0.0611–0.1389), yellow (0.1444–0.1889), green (0.1944–0.4278), cyan (0.4333–0.5500), blue (0.5556–0.6889), purple (0.6944–0.8611), magenta (0.8667–1.0000). Then we count and record the number of points in each category. If the points' quantity of one color is larger than a threshold a, we consider these points as background points. Similarly, if the points' quantity of one color is smaller than a threshold b, we consider these points as noise points. In this paper, a and b are set to 5% and 30% respectively. Both background and noise points should be deleted and the result of point set selection based on color information is shown in Fig. 3.

C. MAXIMUM CORRENTROPY CRITERION BASED REGISTRATION MODEL

In traditional ICP algorithm, the solution of rigid body transformation is described as a LS optimization problem. As shown in Fig. 4(a), the closer the source and target point sets are, the smaller their values are. However, due to the slow

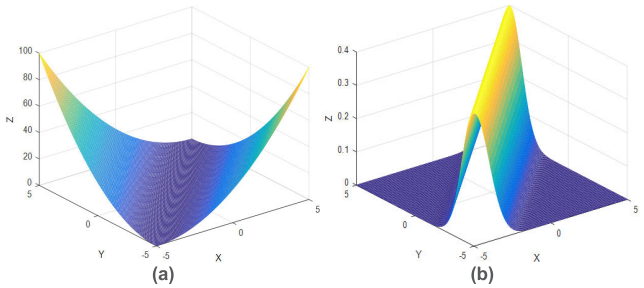

FIGURE 4. Point set selection based on color information. (a) Point set before color screening. (b) Point set after color screening.

rate of change of the square term, the least squares method cannot effectively reduce the impact of noise and outliers on registration accuracy. Coincidentally, as shown in Fig. 3(b), noises and outliers are ubiquitous in a point set after color screening. So even if color information is added, the LS based ICP algorithm still cannot achieve precise registration results. To solve this problem, the maximum correntropy criterion (MCC) is introduced in ICP based algorithm and the MCC can be expressed as follow:

$$g(\vec{x},\vec{y}) = \sum_{i=1}^{N_x} \exp(-||\vec{x}-\vec{y}||_2^2/(2\sigma^2)) \tag{5}$$

where σ is a variance. When the value of σ is small, the curve of Fig.4 (b) is sharp, and it has better robustness to noise and outliers during registration. However, when the value of σ is too small, some correct correspondences will be mistaken for noises and outliers. Therefore, choosing an appropriate value of σ is critical to improving the robustness of the algorithm to noise and outliers. Through a lot of experiments we have found that the best registration results can be achieved by setting the value of σ between 0.4 and 0.6. As shown in Fig. 4(b), the closer the source and target point sets are, the bigger their values are and the rate of change of correntropy is much faster than Least Squares. When solving rigid body transformation, the noises are assigned to smaller weights and the weight of outlier is tend to zero.

Therefore, the MCC based registration algorithm can effectively reduce the impact of noises on registration accuracy and eliminate outliers. Here, the new objective function of MCC based ICP algorithm is [27]:

$$\max_{\mathrm{R},\vec{t},j\in\{1,2,\ldots,N_y\}} \sum_{i=1}^{N_x} \exp(-||\mathbf{R}\vec{x}_i+\vec{t}-\vec{y}_{c_k(i)}||_2^2)/(2\sigma^2))$$
$$s.t.\ \mathbf{R}^T\mathbf{R} = \mathrm{I}_m,\ \det(\mathbf{R}) = 1 \tag{6}$$

Based on this, the objective function after adding color information is:

$$\max_{\mathrm{R},\vec{t},j\in\{1,2,\ldots,N_y\}} \sum_{i=1}^{N_x} \exp\left(-\frac{||\mathbf{R}\vec{x}_i+\vec{t}-\vec{y}_{c_k(i)}||_2^2+w(h_i^x-h_{c_k(i)}^y)^2}{2\sigma^2}\right)$$
$$s.t.\ \mathbf{R}^T\mathbf{R} = \mathrm{I}_m,\ \det(\mathbf{R}) = 1 \tag{7}$$

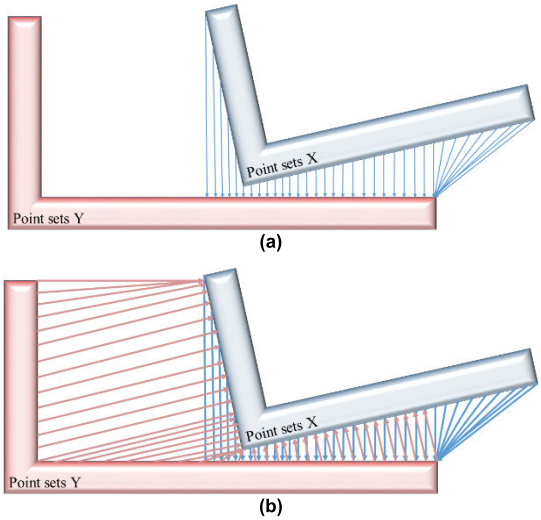

FIGURE 5. Establishing correspondences between two point sets. (a) Establishing correspondences with unidirectional distance measurement. (b) Establishing correspondences with bi-direction distance measurement.

D. BI-DIRECTIONAL DISTANCE MEASUREMENT BASED REGISTRATION MODEL

In ICP algorithm, establishing correspondences is a unidirectional search process from the source point set $X \triangleq \{\vec{x}_i\}_{i=1}^{N_x} (N_x \in \mathbb{N})$ to the target point set $Y \triangleq \{\vec{y}_j\}_{j=1}^{N_y} (N_y \in \mathbb{N})$ as shown in Fig. 5(a). Unidirectional search strategy can build the correspondence effectively, but it may bring ill-pose problem and cause the algorithm to fall into the local extremum sometimes. To solve these issues and improve the robustness of algorithm, the bi-directional distance measurement is introduced into registration framework. Different from unidirectional distance metric, as shown in Fig. 5(b), when the point set X establishes correspondences with the point set Y, the point set Y also establishes correspondences with the point set X at the same time. This method can effectively avoid the algorithm falling into local extremum, thus obtaining a more robust registration results.

Therefore, when the source point set falls into a local extremum when searching for the closest point in the target point set, the correspondences from the target point set to the source point set pull it out of the local extremum and correct this error. The objective function of bi-directional distance measurement based ICP algorithm can be expressed as follows:

$$\min_{\substack{\mathbf{R},\vec{t},\\ c(i)\in\{1,2,\cdots,N_y\}\\ d(j)\in\{1,2,\cdots,N_x\}}} \sum_{i=1}^{N_x} ||(\mathbf{R}\vec{x}_i+\vec{t})-\vec{y}_{c(i)}||_2^2$$
$$+\sum_{j=1}^{N_y} ||(\mathbf{R}\vec{x}_{d(j)}+\vec{t})-\vec{y}_j||_2^2$$
$$s.t.\ \mathbf{R}^{\mathrm{T}}\mathbf{R} = I_m,\ \det(\mathbf{R}) = 1 \tag{8}$$

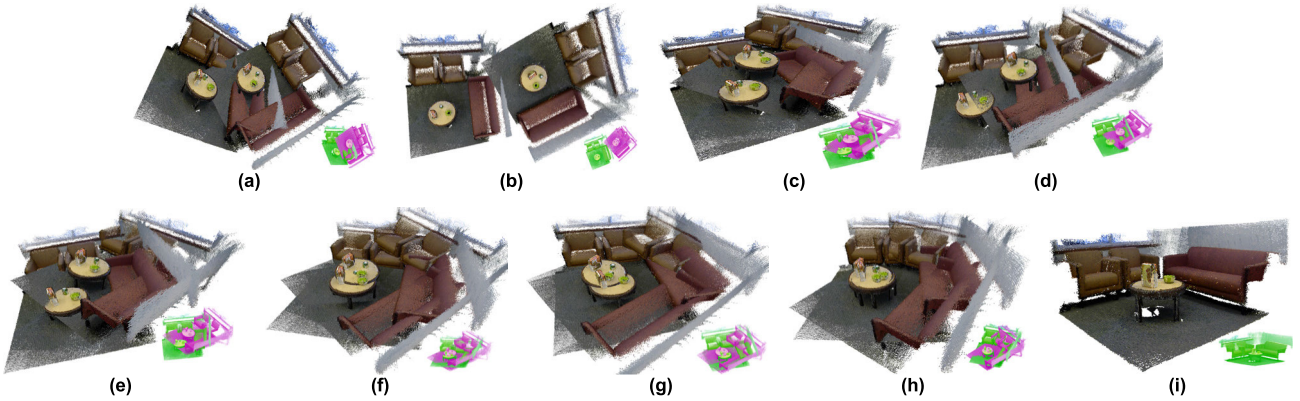

FIGURE 6. Registration results of synthetic test scenes. (a) Initial pose of source and target point sets. (b) Registration result of NDT algorithm. (c) Registration result of ICP algorithm. (d) Registration result of RICP. (e) Registration result of Picky ICP. (f) Registration result of MRICP. (g) Registration result of CICP. (h) Registration result of HCICP. (j) Registration result of the proposed algorithm.

On this basis, combining the color information of the point set and maximum correntropy criterion as mentioned above, the objective function of the proposed point set registration is as follows:

$$\max_{\substack{\mathrm{R},\vec{t}\\ c(i)\in\{1,2,\cdots,N_y\}\\ d(j)\in\{1,2,\cdots,N_x\}}} \exp(-(\sum_{i=1}^{N_x}(||(\mathbf{R}\vec{x}_i+\vec{t})-\vec{y}_{c(i)}||_2^2+w(h_i^x-h_{c(i)}^y)^2) + \sum_{j=1}^{N_y}(||(\mathbf{R}\vec{x}_{d(j)} +\vec{t})-\vec{y}_j||_2^2+w(h_{d(j)}^x-h_j^y)^2))/2\sigma^2)$$
$$s.t.\ \mathbf{R}^T\mathbf{R}=\mathrm{I}_m,\quad \det(\mathbf{R})=1. \tag{9}$$

where $c(\cdot)$ and $d(\cdot)$ are the sets of corresponding points. h_i^x and h_j^y are hues of points in the source and target point sets, w is the weight of hue. $\mathbf{R}$ is a rotation matrix and $\vec{t}$ is a translation vector. σ is a variable to control the convergence rate of maximum correntropy criterion.

IV. THE PROPOSED ALGORITHM

A. THE NEW ICP ALGORITHM

In order to achieve robust point set registration, a new variant of ICP algorithm is given. Being same with standard ICP algorithm, the solving process of the objective function (9) can be divided into two steps

Firstly, building the correspondences with bi-directional distance measurement in k^{th} step:

$$c_k(i)=\arg\min_{c(i)\in\{1,2,\cdots N_y\}}(||(\mathbf{R}_{k-1}\vec{x}_i+\vec{t}_{k-1})-\vec{y}_{c(i)}||_2^2 +w(h_i^x-h_{c(i)}^y)^2) \tag{10}$$

$$d_k(j)=\arg\min_{d(j)\in\{1,2,\cdots N_x\}}(||(\mathbf{R}_{k-1}\vec{x}_{d(j)}+\vec{t}_{k-1})-\vec{y}_j||_2^2 +w(h_{d(j)}^x-h_j^y)^2) \tag{11}$$

Secondly, Calculating the rotation matrix $\mathbf{R}_k$ and translation vector $\vec{t}_k$ in k^{th} step:

$$(\mathbf{R}_k,\vec{t}_k)=\arg\max_{\mathrm{R}^T\mathrm{R}=I_n,\det(\mathrm{R})=1,\vec{t}} \exp(-(\sum_{i=1}^{N_x}(||(\mathbf{R}\vec{x}_i+\vec{t})-\vec{y}_{c_k(i)}||_2^2 + w(h_i^x-h_{c_k(i)}^y)^2)+\sum_{j=1}^{N_y}(||(\mathbf{R}\vec{x}_{d_k(j)}+\vec{t})-\vec{y}_j||_2^2 + w(h_{d_k(j)}^x-h_j^y)^2)))/2\sigma^2) \tag{12}$$

Repeat these two steps until the proposed algorithm reaches the maximum number of iterations or the registration error is less than a set threshold. Normally, we define the maximum number of iterations to be 30, in order to prevent the algorithm from indefinitely iterating.

Being similar to the traditional ICP algorithm, this new ICP algorithm is also a local convergent method. Because of the good resistance of correntropy to noises and outliers and the bi-direction distance measurement broaden the convergence region of the proposed algorithm; this new algorithm can obtain good convergence without easily falling into local extremum.

V. EXPERIMENTAL RESULTS

To verify the robustness of the proposed algorithm, we contrast our algorithm with other registration algorithms, which include ICP [7], DNT [10], CICP [27], RICP [29], Picky ICP [30], HICP [31] and Multi-resolution ICP [32]. Moreover, the comparison algorithm comes from an open source software package named Range Image Registration Toolbox [33]. The algorithm test platform uses an Intel Xeon E5-1650 and a 32.GB RAM. The coding software we used is MATLAB 2018a. In addition, the experimental data come from different public datasets, such as RGB-D scenes dataset v2 (University of Washington) [34], RGB-D SLAM Dataset and Benchmark (Technische Universität München) [35] and NYU Depth Dataset V2 (New York University) [36]. There are 1422 point clouds in Synthetic test scenes and 285 point clouds in Real

TABLE 1. The contrast experiment results of synthetic test scenes.

Data	Error	Algorithms							
		NDT	ICP	RICP	Picky-ICP	MRICP	CICP	HCICP	OURS
Scene1	ε_R	2.1340	6.6290	7.1069	7.4418	$2.40*10^{-05}$	$9.45*10^{-05}$	$1.20*10^{-29}$	$\mathbf{2.77*10^{-30}}$
	$\varepsilon_{\vec{t}}$	2.2859	0.9765	2.4615	3.5298	0.0037	$6.24*10^{-04}$	$1.36*10^{-30}$	$\mathbf{5.89*10^{-31}}$
Scene2	ε_R	2.2232	0.7998	0.6682	0.0240	0.0085	$2.04*10^{-04}$	5.6163	$\mathbf{1.05*10^{-30}}$
	$\varepsilon_{\vec{t}}$	0.3862	0.3061	0.0287	0.0116	0.0147	$4.19*10^{-04}$	14.3968	$\mathbf{1.72*10^{-31}}$
Scene3	ε_R	0.1272	6.3264	4.4203	0.0061	6.6928	0.0024	$1.42*10^{-29}$	$\mathbf{3.81*10^{-30}}$
	$\varepsilon_{\vec{t}}$	0.0884	1.1901	1.0034	$3.91*10^{-04}$	3.2476	$7.82*10^{-04}$	$5.96*10^{-30}$	$\mathbf{1.29*10^{-30}}$
Scene4	ε_R	1.7083	7.4661	6.6536	7.9099	7.8888	0.0014	0.5546	$\mathbf{1.53*10^{-30}}$
	$\varepsilon_{\vec{t}}$	1.1033	4.6272	2.2547	3.9416	4.9157	$8.67*10^{-05}$	0.3844	$\mathbf{6.40*10^{-31}}$
Scene5	ε_R	2.5146	0.1763	0.3781	0.0286	$6.00*10^{-04}$	$5.61*10^{-30}$	$6.45*10^{-30}$	$\mathbf{2.06*10^{-30}}$
	$\varepsilon_{\vec{t}}$	4.2132	0.2601	0.2328	0.1352	0.0040	$1.36*10^{-29}$	$2.69*10^{-30}$	$\mathbf{4.50*10^{-30}}$
Scene6	ε_R	1.8270	1.4098	2.4971	1.6544	0.9149	2.2586	$7.18*10^{-30}$	$\mathbf{2.28*10^{-30}}$
	$\varepsilon_{\vec{t}}$	0.8317	0.1936	0.2447	0.1981	0.3944	1.4795	$8.16*10^{-31}$	$\mathbf{2.06*10^{-31}}$

test scenes. In addition, some real scene data are collected by RGB-D camera. The contrast experiment includes two parts: the test of synthetic scenes and real scenes.

A. SYNTHETIC TEST SCENES

In this subsection, we test the proposed algorithm with synthetic scene data and contrast it with other point set registration algorithms. Before registration, we randomly rotate the source point set along X-axis, Y-axis and Z-axis of 3d coordinate to get the target point set, where the rotation matrix is $\mathbf{R}_1$ and the translation vector is $\vec{t}_1$. Then, we add noises and outliers in point sets randomly. After that, we calculate the rigid transformation matrix $\mathbf{R}_2$ and translation vector $\vec{t}_2$ by registration algorithm and align two point sets according to the matrix. Furthermore, in order to quantify registration accuracy, we use the error of rotation $\varepsilon_{\mathrm{R}} = ||\mathbf{R}_1 - \mathbf{R}_2||_2^2$ and the error of translation vector $\varepsilon_{\vec{t}} = ||\vec{t}_1 - \vec{t}_2||_2^2$ to judge the accuracy of registration. The registration results are shown in Table 1 and Fig. 6. The details of aligned point sets are shown in Fig. 7. In synthetic test scenes, the proposed algorithm requires an average of 14 iterations during registration, which takes an average of 0.258 seconds.

In order to achieve robust point set registration, a new variant of ICP algorithm is given. Being same with standard ICP algorithm, the solving process of the objective function (9) can be divided into two steps.

As shown in Fig. 6 and Table 1, with the interference of noises and outliers and without using the color information of the point sets, the traditional point set registration algorithms cannot establish accurate correspondence, which leads to the reduction of registration accuracy or failure. For CICP algorithm, although the maximum correntropy criterion guarantees the robustness of the algorithm to noises and outliers, it is still unable to align two point sets effectively in most of the time when there is no correct correspondence. Therefore, the proposed algorithm achieves most robustness registration results in synthetic test scenes.

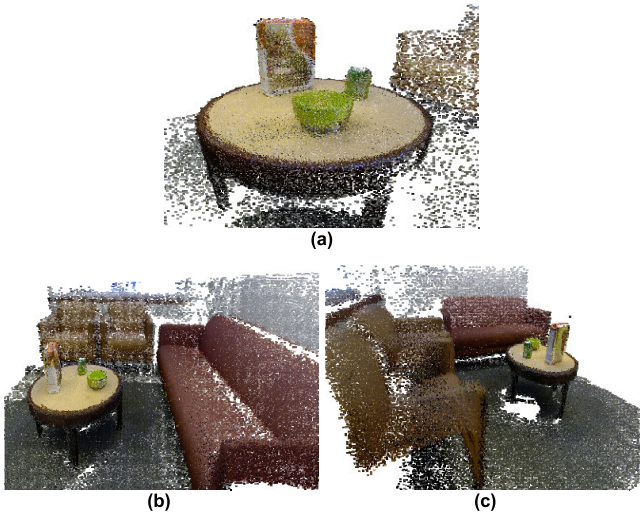

FIGURE 7. Detailed display of registration results of the proposed algorithm. (a) Table. (b) Perspective 1 of the sofa. (c) Perspective 2 of the sofa.

B. REAL TEST SCENES

In this subsection, we test the proposed algorithm with real test data, which are collected by RGB-D camera and the refresh rate of the camera is 30 frames per second. Similarly, we contrast our algorithm with other registration algorithms. Since the rigid transformation between two frames of real scene data is unknown, unlike synthetic data, we can no longer use the error of rotation and translation to measure the accuracy of registration results. Therefore, a new criterion is given to judge the quality of registration results with real test data. In this manuscript, after registering two point sets, we apply the Hausdorff distance to measure the accuracy of

TABLE 2. The contrast experiment results of real test scenes.

Hausdorff distance	Algorithms							
	NDT	ICP	RICP	Picky-ICP	MRICP	CICP	HCICP	Ours
best results	$9.38*10^{-04}$	$5.38*10^{-04}$	$4.12*10^{-04}$	$4.58*10^{-04}$	$5.93*10^{-04}$	$3.37*10^{-04}$	$2.70*10^{-04}$	$2.33*10^{-04}$
next to best results	0.0013	$4.57*10^{-04}$	0.0011	$3.60*10^{-04}$	$5.56*10^{-04}$	$4.81*10^{-04}$	$3.61*10^{-04}$	$2.98*10^{-04}$
next to worst results	0.0015	0.0049	0.018	0.0024	0.0064	0.0172	$8.81*10^{-04}$	0.0016
worst results	0.0236	0.0343	0.1065	0.05	0.0594	0.0533	0.0252	0.0086

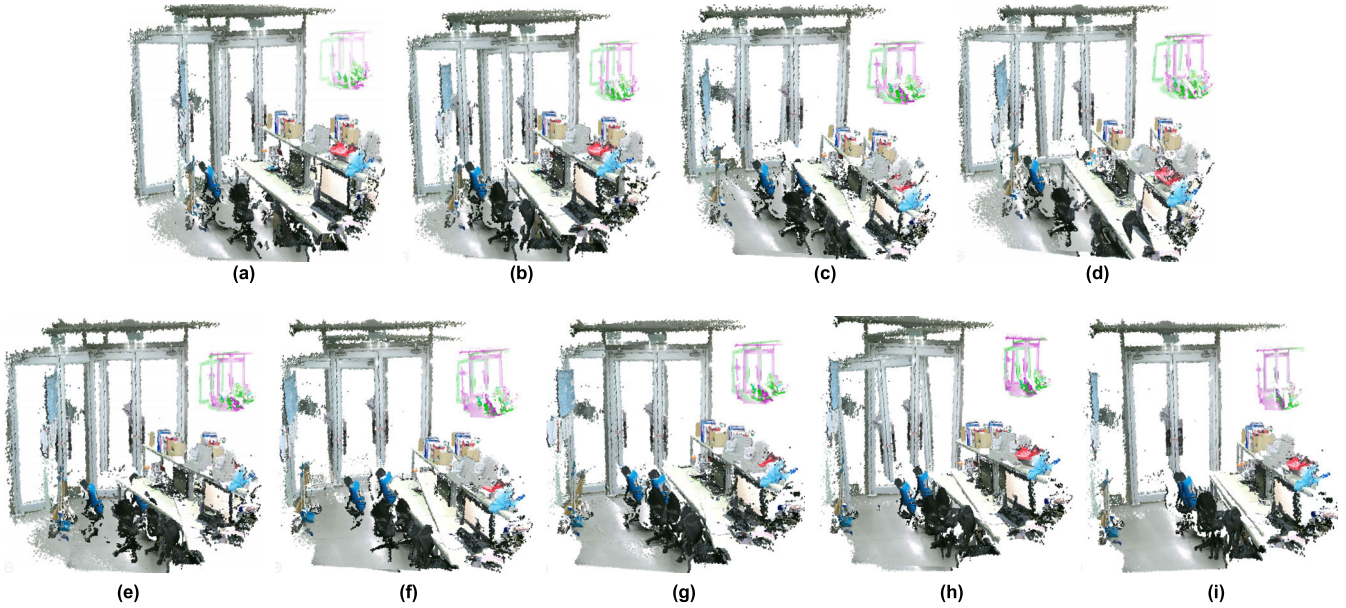

FIGURE 8. Registration results of real test scenes. (a) Initial pose of source and target point sets. (b) Registration result of NDT algorithm. (c) Registration result of ICP algorithm. (d) Registration result of RICP. (e) Registration result of Picky ICP. (f) Registration result of MRICP. (g) Registration result of CICP. (h) Registration result of HCICP. (i) Registration result of the proposed algorithm.

TABLE 3. The convergence time of each registration algorithm.

Algorithms	NDT	ICP	RICP	Picky-ICP
Time (s)	0.1321	0.1270	0.1272	0.1251
Algorithms	MRICP	CICP	HCICP	Ours
Time (s)	0.1249	0.1298	0.1345	0.1283

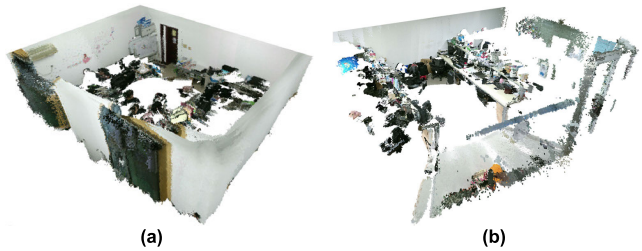

FIGURE 9. Registration results of real test scenes. (a) Initial pose of source and target point sets. (b) Registration result of NDT algorithm.

each registration algorithm. Furthermore, the experimental results of real test data are shown in Table 2 and Fig. 8. In real test scenes, the proposed algorithm requires an average of 5 iterations during registration, which takes an average of 0.081 seconds.

As shown in the experimental results, due to the precise correspondences between two point sets and strong robustness to noises and outliers, the proposed algorithm achieves more accuracy and robust registration results than other algorithms. Meanwhile, we conduct the convergence time of each registration algorithm and the results are shown in Table 3. Furthermore, we apply the proposed algorithm to reconstruct some indoor scenes, and the reconstruction results are shown in Fig. 9.

VI. CONCLUSION

In this paper, a robust point set registration algorithm is proposed to align RGB-D data precisely. Compared with the traditional ICP registration algorithm, this algorithm uses color information and bidirectional distance measurement to establish more accurate and robust correspondence. Meanwhile, we use correntropy to improve the accuracy of registration. As shown in contrast experiments, our algorithm achieves more robustness and accuracy registration results than other rigid registration algorithm.

In addition, we will apply our method for large-scale reconstruction of indoor or door scenes.

APPENDIX

A. THE COMPUTATION OF THE PROPOSED ALGORITHM

To solve (12), we set:

$$F(\mathbf{R},\vec{t}) = \exp(-(\sum_{i=1}^{N_x}(||(\mathbf{R}\vec{x}_i+\vec{t})-\vec{y}_{c_k(i)}||_2^2 + w(h_i^x - h_{c_k(i)}^y)^2) + \sum_{j=1}^{N_y}(||(\mathbf{R}\vec{x}_{d_k(j)}+\vec{t})-\vec{y}_j||_2^2 + w(h_{d_k(j)}^x - h_j^y)^2)))/2\sigma^2) \quad (13)$$

$$m_i = ||(\mathbf{R}\vec{x}_i+\vec{t})-\vec{y}_{c_k(i)}||_2^2 + w(h_i^x - h_{c_k(i)}^y)^2 \quad (14)$$

$$m_j = ||(\mathbf{R}\vec{x}_{d_k(j)}+\vec{t})-\vec{y}_j||_2^2 + w(h_{d_k(j)}^x - h_j^y)^2 \quad (15)$$

and the $F(\mathbf{R},\vec{t})$ can be abbreviated as:

$$F(\mathbf{R},\vec{t}) = \exp(-(\sum_{i=1}^{N_x} m_i + \sum_{j=1}^{N_y} m_j)/2\sigma^2) \quad (16)$$

Calculate the partial derivative of $F(\mathbf{R},\vec{t})$ to $\vec{t}$:

$$\frac{\partial F}{\partial \vec{t}} = -\frac{\sum_{i=1}^{N_x}((\mathbf{R}\vec{x}_i+\vec{t})-\vec{y}_{c_k(i)}) + \sum_{j=1}^{N_y}((\mathbf{R}\vec{x}_{d_k(j)}+\vec{t})-\vec{y}_j)}{\sigma^2} \times e^{-\frac{\sum_{i=1}^{N_x} m_i + \sum_{j=1}^{N_y} m_j}{2\sigma^2}} \quad (17)$$

Set formula (17) to zero and we can get:

$$\vec{t} = \frac{\sum_{i=1}^{N_x}(\vec{y}_{c_k(i)} - \mathrm{R}\vec{x}_i) + \sum_{j=1}^{N_y}(\vec{y}_j - \mathrm{R}\vec{x}_{d_k(j)})}{N_x + N_y} \quad (18)$$

Substitute $\vec{t}$ in (16) and let

$$\vec{p}_i = \frac{(N_x+N_y)\vec{x}_i - \sum_{i=1}^{N_x}\vec{x}_i - \sum_{j=1}^{N_y}\vec{x}_{d_k(j)}}{N_x+N_y} \quad (19)$$

$$\vec{q}_j = \frac{(N_x+N_y)\vec{y}_j - \sum_{i=1}^{N_x}\vec{y}_{c_k(i)} - \sum_{j=1}^{N_y}\vec{y}_j}{N_x+N_y} \quad (20)$$

$$\vec{p}_j = \frac{(N_x+N_y)\vec{x}_{d_k(j)} - \sum_{i=1}^{N_x}\vec{x}_i - \sum_{j=1}^{N_y}\vec{x}_{d_k(j)}}{N_x+N_y} \quad (21)$$

$$\vec{q}_j = \frac{(N_x+N_y)\vec{y}_j - \sum_{i=1}^{N_x}\vec{y}_{c_k(i)} - \sum_{j=1}^{N_y}\vec{y}_j}{N_x+N_y} \quad (22)$$

$$l_i = w(h_i^x - h_{c_k(i)}^y)^2, l_j = w(h_{d_k(j)}^x - h_j^y)^2 \quad (23)$$

and $F(\mathbf{R})$ can be rewritten as:

$$\mathbf{R}_k = \underset{\mathbf{R}^T\mathbf{R}=\mathbf{I}_n,\det(\mathbf{R})=1}{\arg\max} \exp(-(\sum_{i=1}^{N_x}(||\mathbf{R}\vec{p}_i - \vec{q}_i||_2^2 + l_i^2) + \sum_{j=1}^{N_y}(||\mathbf{R}\vec{p}_j - \vec{q}_j||_2^2 + l_j^2)/2\sigma^2) \quad (24)$$

To solve this constrained optimization problem, the Lagrange multiplier method is applied and the new optimized objective function can be written as:

$$L(\mathbf{R},\mathbf{K},\eta) = F(\mathbf{R}) + tr(\mathbf{K}(\mathbf{R}^T\mathbf{R}-\mathbf{I}_n)) + \eta(\det(\mathbf{R})-1) \quad (25)$$

where $\mathbf{K}$ is a Lagrange multiplier and symmetric matrix, η is also a Lagrange multiplier and tr is the trace of the matrix. To maximize the objective function, (25) derives partial derivatives of $\mathbf{R}$, $\mathbf{K}$ and η respectively, and sets the derivative result to zero:

$$\frac{\partial L}{\partial \mathbf{R}} = -\frac{F(\mathbf{R})}{\sigma^2}(\sum_{i=1}^{N_x}(\vec{p}_i\vec{p}_i^T\mathbf{R} - \vec{p}_i\vec{q}_i^T) + \sum_{j=1}^{N_y}(\vec{p}_j\vec{p}_j^T\mathbf{R} - \vec{p}_j\vec{q}_j^T)) + 2\mathbf{K}\mathbf{R} + \eta\mathbf{R} = \mathbf{0} \quad (26)$$

$$\frac{\partial L}{\partial \mathbf{K}} = \mathbf{R}^T\mathbf{R} - \mathbf{I}_n = \mathbf{0} \quad (27)$$

$$\frac{\partial L}{\partial \eta} = \det(\mathbf{R}) - 1 = 0 \quad (28)$$

Let $\mathbf{L}' = -\frac{1}{\sigma^2}F(\mathbf{R})(\sum_{i=1}^{N_x}(\vec{p}_i\vec{p}_i^T) + \sum_{j=1}^{N_y}(\vec{p}_j\vec{q}_j^T)) + 2\mathbf{K} + \eta$ and then we can get:

$$\mathbf{L}'\mathbf{R} = -\frac{1}{\sigma^2}F(\mathbf{R})(\sum_{i=1}^{N_x}(\vec{p}_i\vec{p}_i^T) + \sum_{j=1}^{N_y}(\vec{p}_j\vec{q}_j^T)) \quad (29)$$

In order to simplify the solution, $\mathbf{L}'\mathbf{R}$ is decomposed by singular value decomposition (SVD) method and we can get:

$$\mathbf{L}'\mathbf{R} = \mathbf{U}\mathbf{\Lambda}\mathbf{V}^T \quad (30)$$

here, $\mathbf{U}$ and $\mathbf{V}$ are $n \times n$ unitary matrix, where $\mathbf{\Lambda}$ is a non-negative $n \times n$ dimensional diagonal matrix, and the diagonal elements of matrix $\mathbf{\Lambda}$ are arranged in the order of large to small:$\lambda_1 \geq \lambda_2 \geq \ldots \geq \lambda_{n-1} \geq \lambda_n \geq 0$. By transposing the left and right sides of Formula (28) at the same time, it can be obtained that:

$$\mathbf{R}^T\mathbf{L}'^T = \mathbf{V}\mathbf{\Lambda}\mathbf{U}^T \quad (31)$$

then, left multiplier (31) on the left and right sides of (30), we can get:

$$\mathbf{L}'^2 = \mathbf{U}\mathbf{\Lambda}\mathbf{V}^T\mathbf{V}\mathbf{\Lambda}\mathbf{U}^T \quad (32)$$

by using the same orthogonal matrix reduced to diagonal matrix form, we can get:

$$\mathbf{L}' = \mathbf{U}\mathbf{\Lambda}D(\vec{\mathbf{d}})\mathbf{U}^T \quad (33)$$

$D(\vec{\mathbf{d}})$ is a diagonal matrix $diag(\vec{\mathbf{d}})$, where d_i equals to 1 or -1. On the one hand, (33) shows that:

$$\det(\mathbf{L}') = \det(\mathbf{U}\mathbf{\Lambda}D(\vec{\mathbf{d}})\mathbf{U}^T) = \det(\mathbf{\Lambda})\det(D(\vec{\mathbf{d}})) \tag{34}$$

On the other hand, from (29), we can see that:

$$\det(\mathbf{L}') = \det(\mathbf{L}')\det(\mathbf{R}) = \det(\mathbf{L}'\mathbf{R}) \tag{35}$$

Combine (34) and (35), we can see that:

$$\det(\mathbf{\Lambda})\det(D(\vec{\mathbf{d}})) = \det(\mathbf{L}'\mathbf{R}) \tag{36}$$

In consideration of $\det(\mathbf{\Lambda}) = \lambda_1\lambda_2\ldots\lambda_n \geq 0$, $\det(D(\vec{\mathbf{d}})) = 1$ when $\det(\mathbf{L}'\mathbf{R}) > 0$ and $\det(D(\vec{\mathbf{d}})) = -1$ when $\det(\mathbf{L}'\mathbf{R}) < 0$. Thus, by multiplying the left of equation (31) by $\mathbf{L}'^{-1}$, we can get:

$$\mathbf{R} = (\mathbf{U}\mathbf{\Lambda}D(\vec{\mathbf{d}})\mathbf{U}^T)^{-1}\mathbf{U}\mathbf{\Lambda}\mathbf{V}^T = \mathbf{U}D(\vec{\mathbf{d}})^{-1}\mathbf{V}^T \tag{37}$$

In conclusion, at the k^{th} iteration process, the value of rotation matrix is:

$$\mathbf{R}_k = \mathbf{U}D(\vec{\mathbf{d}})^{-1}\mathbf{V}^T \tag{38}$$

by substituting the result of (26) into (11), the following results can be obtained:

$$\vec{t}_k = \frac{\sum_{i=1}^{N_x}(\vec{y}_{c_k(i)} - \mathbf{R}_k\vec{x}_i) + \sum_{j=1}^{N_y}(\vec{y}_j - \mathbf{R}_k\vec{x}_{d(j)})}{N_x + N_y} \tag{39}$$

REFERENCES

[1] J. Engel, T. Schöps, and D. Cremers, "LSD-SLAM: Large-scale direct monocular SLAM," in *Proc. ECCV*, Zürich, Switzerland, 2014, pp. 834–849.

[2] R. Mur-Artal, J. M. M. Montiel, and J. D. Tardos, "ORB-SLAM: A versatile and accurate monocular SLAM system," *IEEE Trans. Robot.*, vol. 31, no. 5, pp. 1147–1163, Oct. 2015.

[3] S. You, U. Neumann, and R. Azuma, "Hybrid inertial and vision tracking for augmented reality registration," in *Proc. IEEE Virtual Reality*, Houston, TX, USA, Jan. 2003, pp. 260–267.

[4] S.-H. Kong, N. Haouchine, R. Soares, A. Klymchenko, B. Andreiuk, B. Marques, G. Shabat, T. Piechaud, M. Diana, S. Cotin, and J. Marescaux, "Robust augmented reality registration method for localization of solid organs' tumors using CT-derived virtual biomechanical model and fluorescent fiducials," *Surg. Endoscopy*, vol. 31, no. 7, pp. 2863–2871, Jul. 2017.

[5] T. Lehmann, C. Gonner, and K. Spitzer, "Survey: Interpolation methods in medical image processing," *IEEE Trans. Med. Imag.*, vol. 18, no. 11, pp. 1049–1075, Nov. 1999.

[6] Y. Jin, E. Angelini, and A. Laine, "Wavelets in medical image processing: Denoising, segmentation and registration," *Behav. Process.*, vol. 45, nos. 1–3, pp. 33–57, 1970.

[7] P. Besl and N. D. Mckay, "A method for registration of 3-D shapes," *IEEE Trans. Pattern Anal. Mach. Intell.*, vol. 14, no. 2, pp. 239–256, Feb. 1992.

[8] Y. Chen and G. Medioni, "Object modelling by registration of multiple range images," *Image Vis. Comput.*, vol. 10, no. 3, pp. 145–155, Apr. 1992.

[9] Z. Zhang, "Iterative point matching for registration of free-form curves and surfaces," *Int. J. Comput. Vis.*, vol. 13, no. 2, pp. 119–152, Oct. 1994.

[10] P. Biber and W. Strasser, "The normal distributions transform: A new approach to laser scan matching," in *Proc. IEEE/RSJ Int. Conf. Intell. Robots Syst. (IROS)*, Las Vegas, NV, USA, vol. 3, Jul. 2004, pp. 2743–2748.

[11] B. Jian and B. Vemuri, "A robust algorithm for point set registration using mixture of Gaussians," in *Proc. 10th IEEE Int. Conf. Comput. Vis. (ICCV)* Vol. 1, Nov. 2005, pp. 1246–1251.

[12] A. Myronenko and X. Song, "Point set registration: Coherent point drift," *IEEE Trans. Pattern Anal. Mach. Intell.*, vol. 32, no. 12, pp. 2262–2275, Dec. 2010.

[13] P. Wang, P. Wang, Z. Qu, Y. Gao, and Z. Shen, "A refined coherent point drift (CPD) algorithm for point set registration," *Sci. China Inf. Sci.*, vol. 54, no. 12, pp. 2639–2646, Dec. 2011.

[14] M. Bueno, H. González-Jorge, J. Martínez-Sánchez, and H. Lorenzo, "Automatic point cloud coarse registration using geometric keypoint descriptors for indoor scenes," *Autom. Construct.*, vol. 81, pp. 134–148, Sep. 2017.

[15] J. Xie, Y.-F. Hsu, R. S. Feris, and M.-T. Sun, "Fine registration of 3D point clouds with iterative closest point using an RGB-D camera," in *Proc. IEEE Int. Symp. Circuits Syst. (ISCAS)*, Beijing, China, May 2013, pp. 2904–2907.

[16] S.-M. Rhee, Y. B. Lee, and H.-E. Lee, "Two-pass ICP with Color constraint for noisy RGB-D point cloud registration," in *Proc. IEEE Int. Conf. Consum. Electron. (ICCE)*, Shenzhen, China, Jan. 2014, pp. 89–90.

[17] R. Y. Takimoto, M. D. S. G. Tsuzuki, R. Vogelaar, T. D. C. Martins, A. K. Sato, Y. Iwao, T. Gotoh, and S. Kagei, "3D reconstruction and multiple point cloud registration using a low precision RGB-D sensor," *Mechatronics*, vol. 35, pp. 11–22, May 2016.

[18] R. Benjemaa and F. Schmitt, "Fast global registration of 3D sampled surfaces using a multi-Z-buffer technique," *Image Vis. Comput.*, vol. 17, no. 2, pp. 113–123, Feb. 1999.

[19] T. Jost and H. Hügli, "Fast ICP algorithms for shape registration," in *Proc. DAGM*, Zürich, Switzerland, 2002, pp. 91–99.

[20] M. Greenspan and M. Yurick, "Approximate K-D tree search for efficient ICP," in *Proc. 4th Int. Conf. 3-D Digit. Imag. Modeling, 3DIM*, Seattle, WA, USA Jun. 2004, pp. 442–448.

[21] Y. He, B. Liang, J. Yang, S. Li, and J. He, "An iterative closest points algorithm for registration of 3D laser scanner point clouds with geometric features," *Sensors*, vol. 17, no. 8, p. 1862, Aug. 2017.

[22] A. Makovetskii, S. Voronin, V. Kober, A. Voronin, and D. Tihonkih, "Point clouds registration based on the point-to-plane approach for orthogonal transformations," in *Proc. ITNT*, Samara, Russia, 2018, pp. 236–242.

[23] H. Men, B. Gebre, and K. Pochiraju, "Color point cloud registration with 4D ICP algorithm," in *Proc. IEEE Int. Conf. Robot. Autom.*, Shanghai, China, May 2011, pp. 1511–1516.

[24] M. Korn, M. Holzkothen, and J. Pauli, "Color supported generalized-ICP," in *Proc. VISAPP*, Berlin, Germany, 2015, pp. 592–599.

[25] D. Chetverikov, D. Stepanov, and P. Krsek, "Robust Euclidean alignment of 3D point sets: The trimmed iterative closest point algorithm," *Image Vis. Comput.*, vol. 23, no. 3, pp. 299–309, Mar. 2005.

[26] S. Du, J. Liu, C. Zhang, J. Zhu, and K. Li, "Probability iterative closest point algorithm for m-D point set registration with noise," *Neurocomputing*, vol. 157, pp. 187–198, Jun. 2015.

[27] Z. Wu, H. Chen, S. Du, M. Fu, N. Zhou, and N. Zheng, "Correntropy based scale ICP algorithm for robust point set registration," *Pattern Recognit.*, vol. 93, pp. 14–24, Sep. 2019.

[28] S. Du, G. Xu, S. Zhang, X. Zhang, Y. Gao, and B. Chen, "Robust rigid registration algorithm based on pointwise correspondence and correntropy," *Pattern Recogn. Lett.*, to be published.

[29] E. Trucco, A. Fusiello, and V. Roberto, "Robust motion and correspondence of noisy 3-D point sets with missing data," *Pattern Recognit. Lett.*, vol. 20, no. 9, pp. 889–898, Sep. 1999.

[30] T. Zinsser, J. Schmidt, and H. Niemann, "A refined ICP algorithm for robust 3-D correspondence estimation," in *Proc. Int. Conf. Image Process.*, vol. 2, Sep. 2003, pp. II–695.

[31] T. Wan, S. Du, Y. Xu, G. Xu, Z. Li, B. Chen, and Y. Gao, "RGB-D point cloud registration via infrared and color camera," *Multimedia Tools Appl.*, vol. 78, no. 23, pp. 33223–33246, Dec. 2019.

[32] T. Jost and H. Hugli, "A multi-resolution ICP with heuristic closest point search for fast and robust 3D registration of range images," in *Proc. 4th Int. Conf. 3-D Digit. Imag. Modeling, 3DIM*, Banff Town, AB, Canada Jun. 2004, pp. 427–433.

[33] J. Salvi, C. Matabosch, D. Fofi, and J. Forest, "A review of recent range image registration methods with accuracy evaluation," *Image Vis. Comput.*, vol. 25, no. 5, pp. 578–596, May 2007.

[34] K. Lai, L. Bo, X. Ren, and D. Fox, "A large-scale hierarchical multi-view RGB-D object dataset," in *Proc. IEEE Int. Conf. Robot. Autom.*, San Francisco, CA, USA, May 2011, pp. 1817–1824.

[35] J. Sturm, N. Engelhard, F. Endres, W. Burgard, and D. Cremers, "A benchmark for the evaluation of RGB-D SLAM systems," in *Proc. IEEE/RSJ Int. Conf. Intell. Robots Syst.*, Vilamoura, Portugal, Oct. 2012, pp. 573–580.

[36] N. Silberman, D. Hoiem, P. Kohli, and R. Fergus, "Indoor segmentation and support inference from RGBD images," in *Proc. ECCV*, Florence, Italy, 2012, pp. 746–760.

TENG WAN received the bachelor's degree in electrical engineering and automation and the master's degree in power system and automation from the Lanzhou University of Technology, in 2012 and 2017, respectively. He is currently pursuing the Ph.D. degree in control science and engineering from Xi'an Jiaotong University. His research interests include computer vision and pattern recognition.

SHAOYI DU received the B.S. degree in computational mathematics and computer science, the M.S. degree in applied mathematics, and the Ph.D. degree in pattern recognition and intelligence system from Xi'an Jiaotong University, China in 2002, 2005, and 2009, respectively. He worked as a Postdoctoral Fellow with Xi'an Jiaotong University from 2009 to 2011 and visited the University of North Carolina at Chapel Hill from 2013 to 2014. He is currently a Professor with the Institute of Artificial Intelligence and Robotics, Xi'an Jiaotong University. His research interests include computer vision, machine learning, and pattern recognition.

WENTING CUI received the B.S. degree in computer science and technology from Tiangong University, in 2015, and the M.S. degree from the School of Software Engineering, Xi'an Jiaotong University, in 2019. She is currently pursuing the Ph.D. degree in control science and engineering from Xi'an Jiaotong University. Her research interests include computer vision, pattern recognition, and medical image analysis.

YANG YANG received the B.E. degree in information engineering from Xi'an Jiaotong University, China, in 2005, and the Double Ph.D. degrees in pattern recognition and intelligent system from Xi'an Jiaotong University, China, and in systems innovation engineering from Tokushima University, Japan, in 2011. She is currently an Associate Professor with the School of Electronic and Information Engineering, Xi'an Jiaotong University, China. Her research interests include image processing, multimedia, and machine learning.

CE LI received the Ph.D. degree in pattern recognition and intelligence system from Xi'an Jiaotong University, China, in 2013. He is currently a Professor with the College of Electrical and Information Engineering, Lanzhou University of Technology. His research interests include computer vision and pattern recognition.